EARTH'S CRYOSPHERE
SCIENTIFIC JOURNAL

Earth's Cryosphere, 2021, vol. XXV, No. 6, pp. 34–41 http://earthcryosphere.ru/

GEOLOGICAL CRYOGENIC PROCESSES AND FORMATIONS

THE INVENTORY OF RETROGRESSIVE THAW SLUMPS (THERMOCIRQUES) IN THE NORTH OF WEST SIBERIA BASED ON 2016–2018 SATELLITE IMAGERY MOSAIC

N.B. Nesterova[1], A.V. Khomutov[1,2], M.O. Leibman[1,2], T.A. Safonov[1], N.G. Belova[2,3]

[1] *Tyumen State University, Volodarskogo str. 6, Tyumen, 625003, Russia; n.b.nesterova@utmn.ru*
[2] *Earth Cryosphere Institute, Tyumen Scientific Centre SB RAS, Malygina str. 86, Tyumen, 625026, Russia; akhomutov@gmail.com*
[3] *Lomonosov Moscow State University, Faculty of Geography, Leninskiye Gory 1, Moscow, 119991, Russia; belova@geogr.msu.ru*

Remote sensing methods of retrogressive thaw slumps (RTS) – also called thermocirques (TC) – study include identification of them on vast territories. The satellite imagery mosaics from the Yandex.Maps service covering the Yamal and Gydan peninsulas was innovatively used for this purpose. All RTS (TC) that occurred at the lake coasts were classified as either active or stabilized, the orientation of each RTS (TC) was determined. We identified 86 active and 20 stabilized RTS in the Yamal peninsula and 224 active and 109 stabilized RTS in Gydan. The distribution of RTS orientation was found to be not random. Multiple comparisons of RTS orientation over cardinal compass points showed a statistically significant predominance of the Northern RTS orientation over the Eastern, as well as the Western orientation over the Eastern. At the same time, none of the orientations showed statistically significant predominance over the others. No statistically significant relationship between RTS orientation and RTS activity was found.

Keywords: *thermodenudation, thermocirques, retrogressive thaw slumps, remote sensing, statistics, Yamal, Gydan, Yandex.Maps.*

INTRODUCTION

Thermodenudation is a complex of slope and erosion processes associated with the thawing of exposed permafrost or ground ice [*Kizyakov, 2005*].

Continuous distribution of permafrost and the presence of tabular ground ice [*Baulin et al., 1967; Romanenko et al., 2001*], in combination with the dynamics of the active layer [*Leibman, Egorov, 1996*], contribute to the development of thermodenudation and formation of specific negative landforms [*Voskresensky, 2001; French, 2017*]. In English-language literature, thermodenudation landforms, as well as the process contributing to their development, are described by the term *retrogressive thaw slump* (RTS) [*Burn, Friele, 1989; French, 2017*]. Thermodenudation developing inland differs from that on the seashores by coastal thermoerosion added [*Khomutov, Leibman, 2008*]. In this work, the subject of this study is thermodenudation landforms located inland and confined to lakeshores: thermocirques (TC) or in other words retrogressive thaw slumps (RTS), which, according to the classification of M.O. Leibman and A.I. Kizyakov [*2007*], formed by a complex of cryogenic earth flows of different ages.

RTS or TC have the shape of a crescent depression in the slope, developing polycyclically through activation and stabilization stages, and becoming more active at intervals of several years [*Burn, 2000*]. A characteristic element of the active RTS morphology is the presence of a sub-vertical headwall with ice or ice-rich permafrost exposure, as well as flows of wet material [*Lewkowicz, 1987; Lantuit, Pollard, 2005*]. During the stabilization stage, RTS (TC) stabilize and overgrow [*Burn, Friele, 1989*], while the outline of the headwall of once active RTS is visible in the relief [*Brooker et al., 2014*].

RTS (TC) are under study by both field and remote-sensing methods. Due to their polycyclic nature, it is important to study the long-term dynamics of RTS [*Lewkowicz, Way, 2019*].

An important area of RTS (TC) research method using remote sensing is their inventory: identification of all RTS found in the imagery and the parameters such as orientation, activity status, size, polycyclicity, etc. Multispectral satellite imagery [*Kokelj et al., 2013; Lacelle et al., 2015*], as well as aerial photographs, are used to look for RTS [*Segal et al., 2016*]. Among the methods of direct identification of RTS using imagery, the following can be highlighted:

– visual manual digitization based on characteristic features [*Kokelj et al., 2013; Ramage et al., 2017; Lewkowicz, Way, 2019*];

– automated interpretation of satellite imagery (tasselled cap) [*Brooker et al., 2014*];

– deep learning method [*Huang et al., 2020*].

For further study of identified RTS, regression analysis is often used [*Lacelle et al., 2015; Segal et al., 2016; Ramage et al., 2017*] as well as correlation analysis [*Balser et al., 2014*] testing the influence of various environmental controls on the formation and polycyclic behaviour of RTS. In some works, different activity stages are also considered [*Balser et al., 2014; Ramage et al., 2017*]. A limited number of studies provide data on the RTS orientation or the orientation of the slope with RTS [*Kokelj et al., 2009; Lacelle et al., 2015; Wang et al., 2016*].

There is no database of RTS (TC) distribution in the Arctic, and there are no large-scale maps of the tabular ground ice distribution in the north of West Siberia, while tabular ground ice is a key factor in RTS occurrence in West Siberia. Satellite imagery makes it possible to cover vast areas, identify a large number of RTS and perform statistical processing of their distribution and various parameters. At the same time, the application of satellite imagery not only as commonly used raster files but also as a mosaic of satellite imagery in the background of available online cartographic services has great potential.

This study is aimed at making an inventory of RTS located inland of the peninsulas (RTS on the seacoasts were not considered here) and occurring at lake catchments. It is based on the only freely available mosaic of high-resolution satellite imagery of 2016–2018, presented on the Yandex.Maps online service (http://yandex.ru/maps). Additionally, primary statistical analysis of the relationship between the number of RTS, their activity and orientation was performed. The Yamal and Gydan peninsulas were selected as the study area, field observations of RTS being undertaken at the key sites, while their large-scale inventory was never performed.

STUDY AREA

The study covers the north of West Siberia within an area between 68–72° N and 66–83° E. The study area is an accumulation plain. Further from the coasts in the north of the peninsulas elevations of 35 m above sea level are observed. A significant part of central Yamal is a flat and rolling hills surface with elevations up to 67 m above sea level. The Yuribey Upland along the Gydan coast has elevations up to 87 m above sea level. The Gydan ridge stretches in its central part from southwest to northeast, with elevations up to 127 m above sea level [*Ecological atlas..., 2018*]. The peninsulas are characterized by ravine-gully and small river networks complicated by thermoerosion and thermokarst landforms [*Romanenko, 1997; Gubarkov, Leibman, 2010*]. There are plenty of bogs and lakes. The majority of the lakes are classified as thermokarst and oxbow [*Romanenko, 1997*]. Recent studies have stated the possibility that some lakes result from intense gas emissions [*Dvornikov et al., 2019*].

The territory is characterized by continuous permafrost distribution, permafrost thickness reaches 450 m [*Ershov, 1989*]. The specificity of the studied peninsulas is the widespread tabular ground ice [*Streletskaya et al., 2002*] and its shallow occurrence, which determines the presence of numerous RTS [*Khomutov et al., 2012*].

MATERIALS AND METHODS OF RTS (TC) IDENTIFICATION

The work includes identification of RTS (TC), the status of their activity, RTS orientation, and statistical analysis.

Identification of RTS (TC) and their activity status

The identification of the RTS (TC) located inland and occurring at the lake coasts on the Yamal and Gydan peninsulas was done manually on the Yandex.Maps online service (http://yandex.ru/maps) by creating a point with a spatial reference. We used visual interpretation signs. For each point, information on RTS activity status and orientation was added.

Satellite data for imagery mosaics, available at the online service Yandex.Maps were processed by the SCANEX company using databases: WorldView-2 Data (DigitalGlobe, Inc.), IKONOS Data (Geo Eye, Inc.), TerraColor Data (Earthstar Geographics), IRS Data (ANTRIX Corporation Ltd.), European Space Imaging GmBH data, DigitalGlobe, Inc. and Airbus DS. These databases contain imagery from WorldView-2, IKONOS, Landsat-7, Sentinel, SPOT-1-5 and many others.

The Yandex.Maps service does not provide information on the time and date of the survey, as well as on the satellite model used for specific satellite imagery from the mosaics. This limits the possibilities of detailed analysis, as well as the study of the spectral characteristics of objects, but did not exclude the possibility of identifying RTS by visual interpretation signs. Therefore, the lack of detailed information about the time and date of the survey and satellite model does not seem crucial. At the same time, the People's Yandex.Maps service, which shows the same mosaic of satellite imagery as on the Yandex.Maps service, provides information on the month and year of the survey. Satellite imagery of the study area was taken mainly in July 2017, partially in July 2016, September 2016, June 2017 and September 2017. Our work was carried out after updating the mosaic of satellite imagery presented in the database covering the study area in 2018.

It should be highlighted that objects identified as RTS, were retrieved using imagery presented in the Yandex.Maps service with different spatial resolution ranging from 0.4 to 15 m, mainly up to 2 m. In this regard, only relatively large RTS (with a length

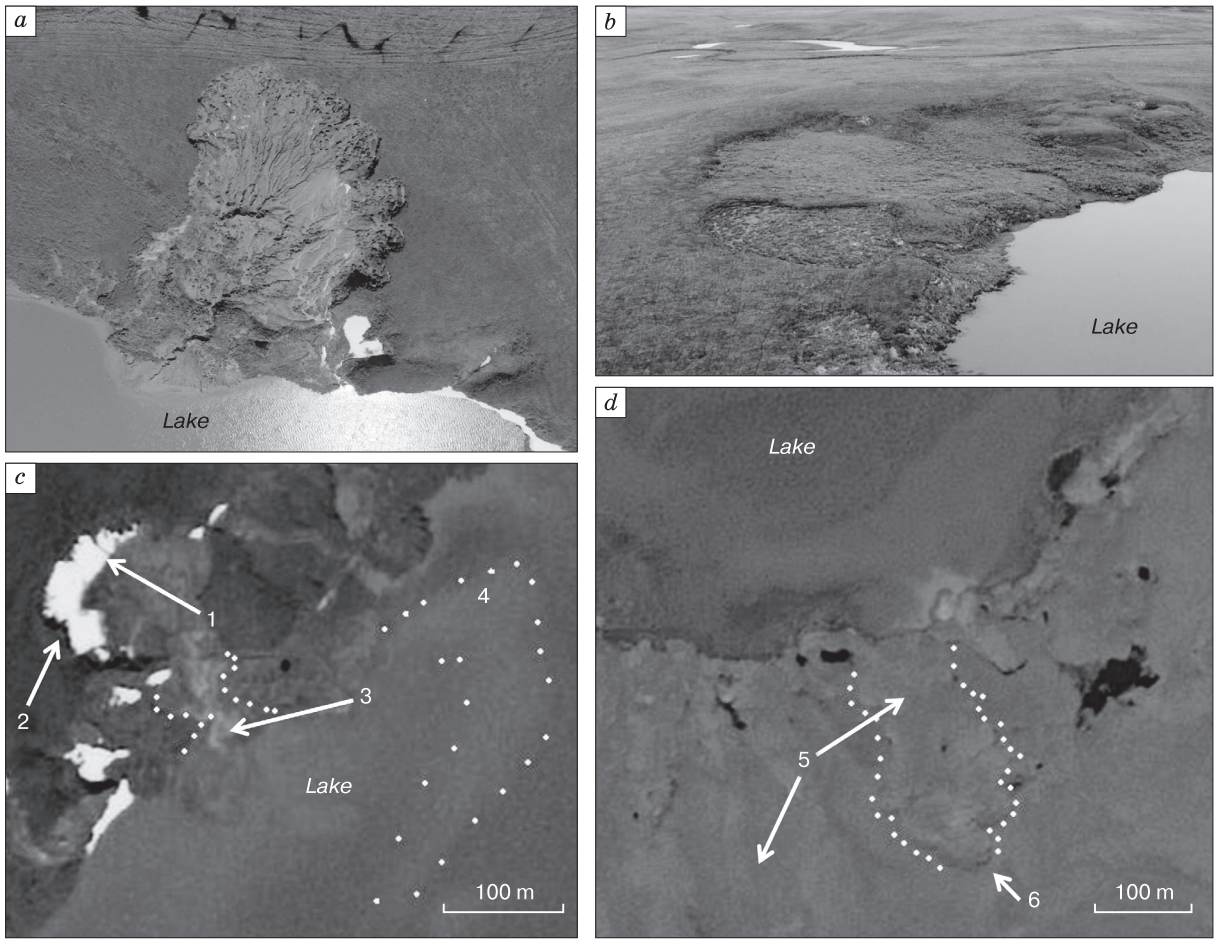

Fig. 1. Examples of RTS (TC) and their visual interpretation signs:

a – an active RTS, a photo taken from an unmanned aerial vehicle (photo by A.V. Khomutov); *b* – stabilized RTS, a photo taken from an unmanned aerial vehicle (photo by A.V. Khomutov); *c* – an active RTS in a mosaic of satellite imagery from Yandex.Maps; visual interpretation signs: *1* – a specific crescent shape, *2* – snow and (or) shadow, outlining RTS headwall, *3* – a flow of thawed grey material (outlined by a dotted line) [*Segal et al., 2016*], *4* – increased water turbidity and a tail of thawed grey material (outlined by a dotted line); *d* – a stabilized RTS in a mosaic of satellite imagery from Yandex.Maps; visual interpretation signs: *5* – RTS colour similar to the colour of the surrounding tundra vegetation; *6* – a noticeable edge of the former headwall (outlined by a dotted line).

and width of at least 20 m) were considered, their identification was doubtless.

RTS (TC) were divided into two groups according to their activity: active and stabilized. Examples of an active and stabilized RTS (TC) on the photos taken from an unmanned aerial vehicle are shown in Fig. 1. Typical visual interpretation signs of active RTS (TC) on satellite imagery are: a crescent shape of a pronounced edge, the presence of a headwall with exposures of permafrost and tabular ground ice, a snowpack or shadow that outlines headwall, flows of thawed material, and the absence of vegetation [*Balser et al., 2014; Brooker et al., 2014; Segal et al., 2016*]. Stabilized RTS (TC) are visually characterized by the absence of a headwall with exposures of permafrost and tabular ground ice (shadow from the scarp), the absence of flows of thawed material (grey colour), the presence of vegetation (green colour), while the relief of the former exposure is noticeable [*Balser et al., 2014; Brooker et al., 2014*]. The interpretation signs of active and stabilized RTS on the mosaic of satellite imagery of the Yandex.Maps service are shown in Fig. 1, *c*, *d*. Partially stabilized RTS with some signs of activity (for example, flows) are classified as active.

To assess the effectiveness of the use of visual interpretation signs, the authors superimposed RTS marked on very-high-resolution satellite imagery available for some areas to RTS on Yandex.Maps service image and received a satisfactory result (Fig. 2).

Further visualization and analysis of the obtained georeferenced point data were performed in the ArcGIS 10.3 program.

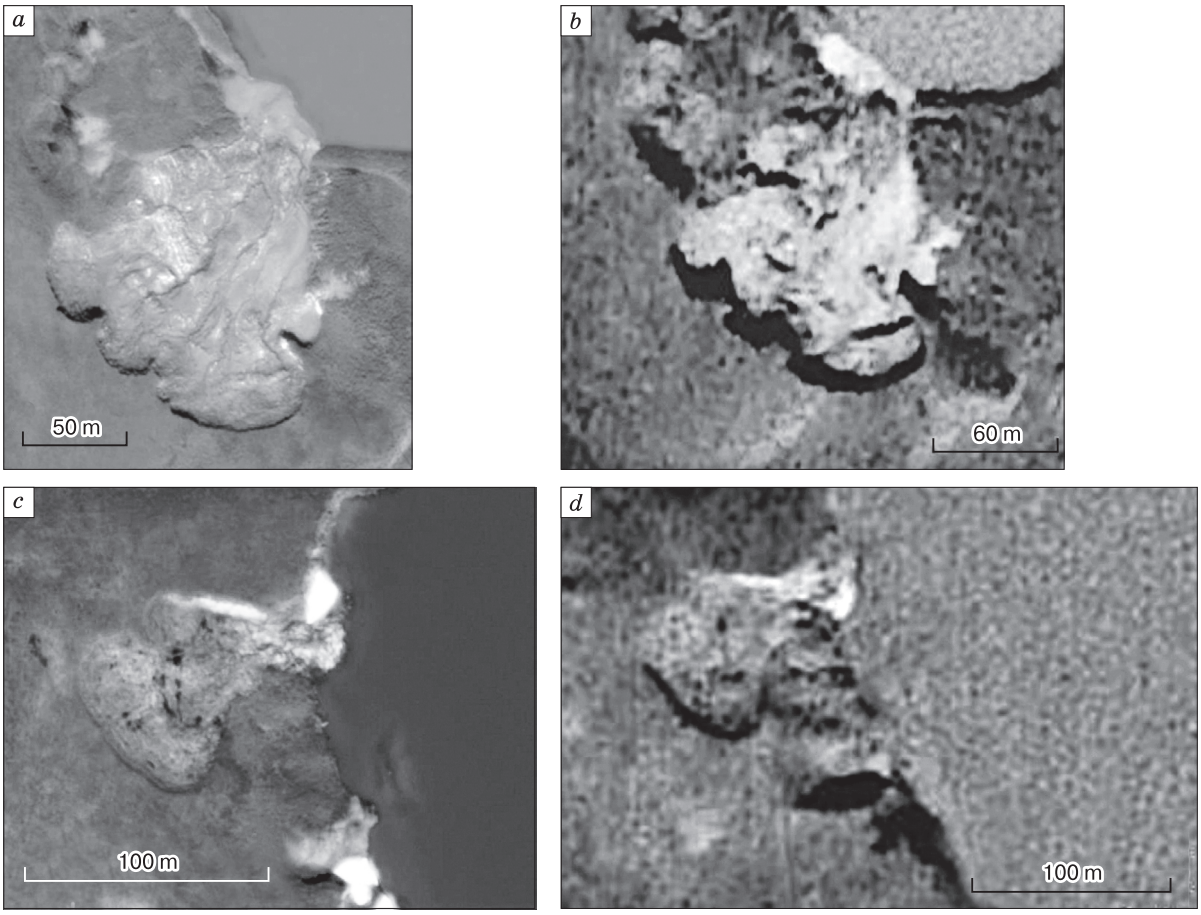

Fig. 2. Examples of an active RTS (*a*, *b*) and a stabilized RTS (*c*, *d*) in the WorldView-2 satellite imagery dated July 10, 2018 (*a*, *c*) and a mosaic of satellite imagery from the Yandex.Maps service, 2018 (*b*, *d*).

RTS orientation and statistical analysis

There is no generally accepted idea of what is RTS orientation. In some studies, RTS orientation is defined as the slope orientation [*Lacelle et al., 2015*], the orientation of the headwall [*Wang et al., 2016*], or as the direction of the normal to the line between two points of intersection of RTS edges with the shoreline of the lake [*Kokelj et al., 2009*]. The authors accepted the last one from [*Kokelj et al., 2009*]. The chosen method allows us to compare our results with the results obtained in the north of Canada (Fig. 3).

RTS orientation initially was determined along 16 points of the compass. For further comparison of the obtained results with the data in [*Kokelj et al., 2009*], orientations were combined into cardinal compass points: N, S, W, and E.

To determine whether the distribution of RTS orientation is random, we used the Pearson's goodness-of-fit test (chi-squared test for equal proportions), which was also applied in [*Kokelj et al., 2009*]. Pearson's goodness-of-fit test is used to assess the correspondence of an empirical distribution to a theo-

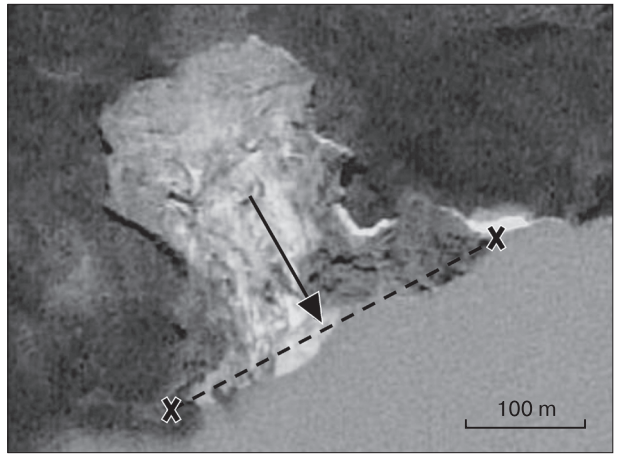

Fig. 3. Visualization of the method for determining RTS orientation [*Kokelj et al., 2009*].

The "X" symbol denotes the point of intersection of RTS edges with the shoreline of the lake, the dashed line connects the two points of intersection, and the arrow is perpendicular to this line (the direction of the arrow is accepted for the RTS orientation).

retical one [*Stepanov, Shavrin, 2005*]. In our case, the theoretical is a uniform distribution. Any statistically significant deviation of the distribution of RTS orientations from the theoretical one is considered uneven, thus, not random.

To determine the regularity of the distribution of RTS orientations over cardinal compass points, and to detect the predominance of one of them over the others, a multiple (pairwise) comparison of exposures with each other was carried out using a test for equal proportions. As a result, Fisher's *z*-test was calculated. This allowed us to calculate the *p*-value with a threshold value of 5 %.

To determine the relationship between activity status and RTS orientation, Pearson's goodness-of-fit test was applied as well.

All statistical tests were performed using RStudio v.1.2.5001 software.

RESULTS AND DISCUSSION

On the Yamal and Gydan peninsulas, 439 RTS were identified on a total area of ~88 thousand km^2, i.e., about 5 RTS per 1000 km^2. On Yamal with a total area of 122 thousand km^2, 106 RTS are located on an area of ~40.8 thousand km^2, i.e., less than 3 per 1000 km^2. On Gydan with a total area of 160 thousand km^2, 333 RTS are found on an area of ~47.2 thousand km^2, i.e., more than 7 per 1000 km^2.

On Yamal, we have identified 86 active and 20 stabilized RTS. On Gydan, 224 RTS active and 109 stabilized RTS were found (Fig. 4).

Since only relatively large RTS were identified, we initially underestimated the total number of RTS of different sizes on both peninsulas. Other researchers also note the likelihood of underestimating the number of RTS during the manual procedure on the imagery of medium spatial resolution [*Lewkowicz, Way, 2019*].

The northernmost RTS on Yamal is located at 70°56′14″ N, the southernmost – at 68°00′55″ N. On Gydan, the northernmost RTS is located at 71°56′25″ N, the southernmost at 69°25′09″ N. The area of RTS distribution is located within the zone where tabular ground ice was observed and described (Fig. 4) [*Streletskaya et al., 2002*], which, along with ice-rich permafrost and ice wedges, determines the occurrence of thermodenudation landforms in this

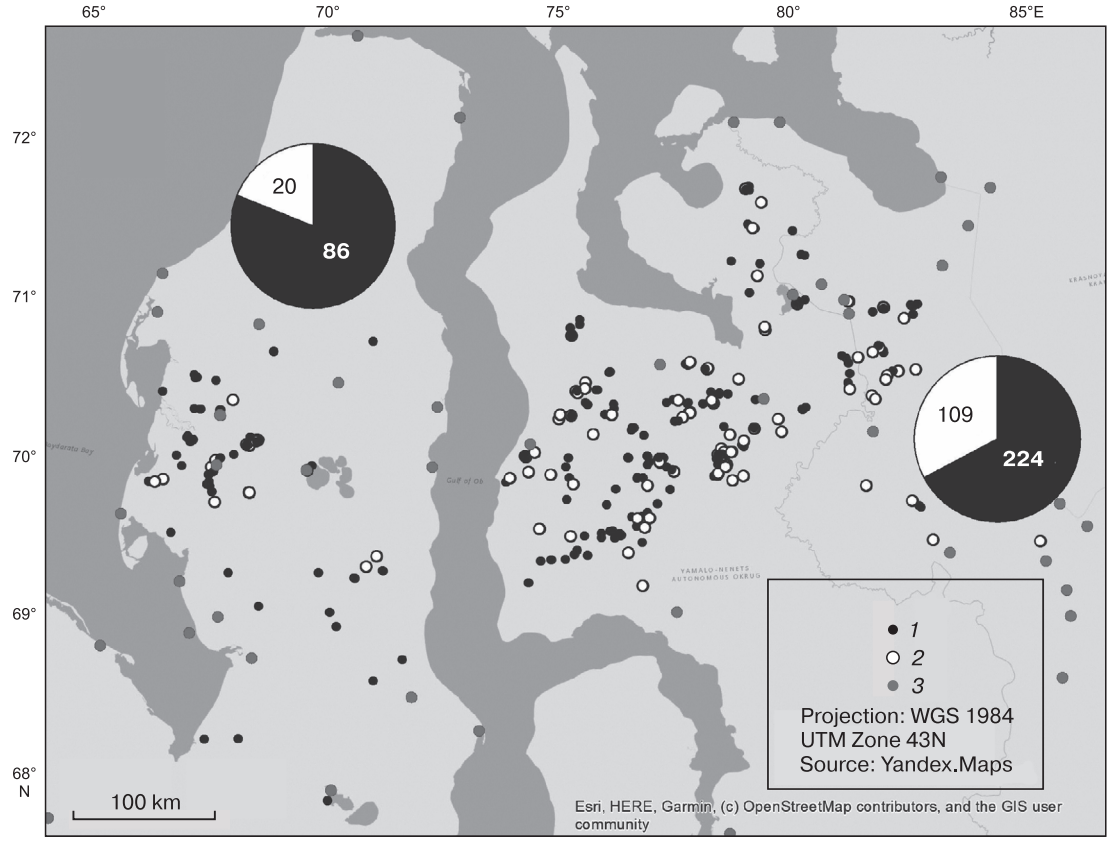

Fig. 4. Distribution of the identified RTS on the Yamal and Gydan peninsulas.

1 – active RTS; *2* – stabilized RTS; *3* – sites of tabular ground ice occurrence, indicated in the publications of the "Massive ice" database [*Streletskaya et al., 2002*]. The pie charts show the number of identified RTS of the different activity statuses on the Yamal and Gydan peninsulas.

region. The presence of tabular ground ice in the north of the Yamal Peninsula does not lead to the development of RTS due to a significant decrease in the terrain elevations there.

The predominance of active RTS on both peninsulas shows that in 2016–2018 thermodenudation processes were actively progressing in the study area (Fig. 4). This is consistent with the results of field studies in this area [*Khomutov et al., 2017*].

The distribution of RTS orientation for Yamal and Gydan is shown in Fig. 5.

In general, for both peninsulas, the statistical test showed that at the 5 % significance level, the distribution of RTS orientations over cardinal compass points is not random. This conclusion is consistent with the results obtained in the study by S. Kokelj et al. [*2009*] discussing the distribution of 530 RTS (both active and stabilized) in the highlands east of the Mackenzie River (northern Canada). In our study, none of the RTS orientations was determined as statistically predominant over all the others. It should be highlighted that multiple comparisons of RTS orientations showed a statistically significant predominance of northern orientation over eastern, as well as a western orientation over eastern. There is also no correlation at the 5 % level of significance between the RTS orientation in total on both peninsulas and the status of RTS activity.

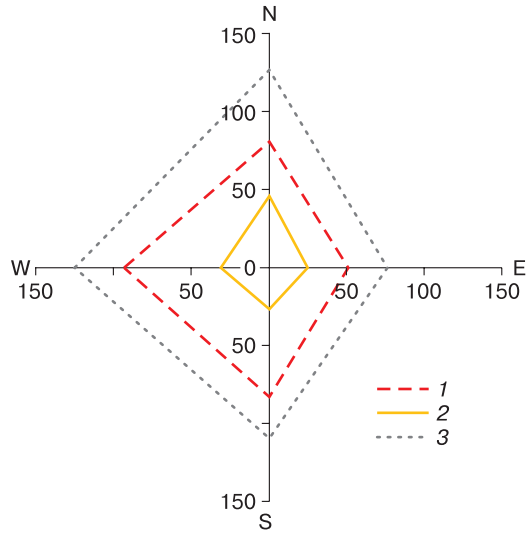

Fig. 5. Distribution of RTS orientation by cardinal compass points in Yamal and Gydan.

Number of RTS: *1* – active, *2* – stabilized, *3* – total active and stabilized.

From the given sample on each of the peninsulas, differences in the distribution of orientations of active and stabilized RTS were revealed. Despite the

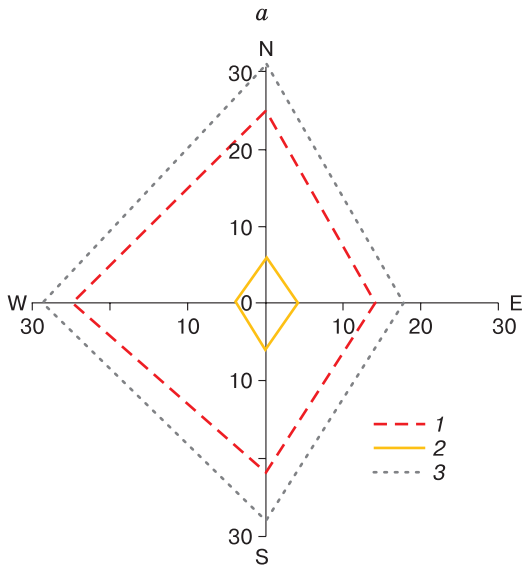

Yamal

Cardinal direction	Number of RTS		
	1	*2*	*3*
N	25	6	31
E	14	4	18
S	22	6	28
W	25	4	29

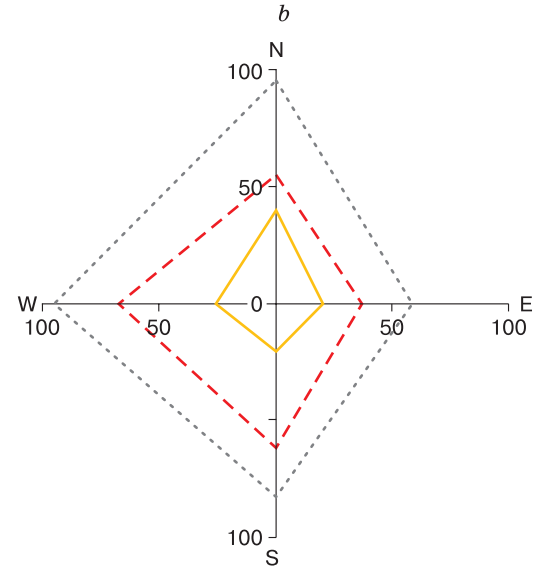

Gydan

Cardinal direction	Number of RTS		
	1	*2*	*3*
N	56	40	96
E	38	21	59
S	62	21	83
W	68	27	95

Fig. 6. Distribution of RTS orientation by cardinal compass points in Yamal (*a*) and Gydan (*b*).

For legend see Fig. 5.

similar distribution of orientations of all RTS on both peninsulas (Fig. 6), active RTS on Yamal have predominant northern, western, and southern orientations, and on the Gydan Peninsula – southern and western. For the stabilized RTS on Yamal, there is no prevailing orientation, and for Gydan, it is clearly defined to face the north.

Similar studies showed that in northwestern Canada (Richardson Ridge and Peel Plateau), eastern orientations prevail for 212 RTS observed [*Lacelle et al., 2015*]. In northwestern Canada (the Mackenzie River delta), the prevailing orientation of RTS was identified as northern [*Kokelj et al., 2009*], and a study of 18 RTS located in northern Canada demonstrated that RTS development was not related to slope orientation [*Wang et al., 2016*].

Such ambiguous results concerning the prevalence of any RTS orientation with different activity statuses are probably related to the presence of other driving factors that were not considered in this paper. Such factors can be geological and geocryological features (ice content in permafrost, depth to the tabular ground ice, distribution of active layer thickness on slopes of different orientations); climatic controls (thickness of snow on slopes of different orientations, duration of sunshine, wind direction); geomorphology (predominance in the particular orientation of slopes in the study area); biogeographic characteristics (shrub height) of RTS sites. All these factors are to be considered in a further much more detailed study of the RTS distribution in the north of West Siberia.

CONCLUSION

In this work, the method of visual identification of RTS (TC) based on a mosaic of publicly available satellite imagery of the Yandex.Maps cartographic service was successfully applied for the first time to the area of the Yamal and Gydan peninsulas.

As a result, 439 RTS were discovered: 106 RTS located on Yamal (86 active and 20 stabilized), and 333 RTS located on Gydan (224 active and 109 stabilized).

The northernmost and southernmost RTS identified on the Yamal Peninsula are located at 70°56′14″ N, and 68°00′55″ N, respectively, and identified on the Gydan Peninsula, at 71°56′25″ N, and 69°25′09″ N, respectively.

The revealed predominance of active RTS is consistent with the results of the field studies of the authors who reported the intensification of thermodenudation in recent years in connection with the extreme climatic events of 2012 and 2016.

The primary statistical analysis of RTS orientation showed: 1) non-random distribution of RTS orientations with a significance level of 5 %, while none of the directions was noted as prevailing over all the others, in other words, there was no dominant RTS orientation found; 2) the absence of a statistically significant relationship between RTS orientation and the status of their activity.

The results are partially consistent with the results of studies in the north and northwest of Canada, where thermodenudation processes are widespread, and the differences are probably related to the regional geological-geomorphological, geocryological, cryolithological, environmental and climatic characteristics of the study area.

The results obtained demonstrate the widespread distribution of RTS in the study area, and their successful inventory based on publicly available remote sensing materials provides a basis for their further multifactorial research.

Acknowledgements. *This work was carried out with partial financial support from the Russian Foundation for Basic Research within the framework of scientific project No. 18-05-60222. Methodological approaches were developed when performing work on state assignment No. 121041600042-7.*

References

Balser, A.W., Jones, J.B., Gens, R., 2014. Timing of retrogressive thaw slump initiation in the Noatak Basin, northwest Alaska, USA. J. Geophys. Research: Earth Surface, CXIX (5), 1106–1120.

Baulin, V.V., Belopukhova, E.B., Dubikov, G.I., Shmelev, L.M., 1967. Geocryological Conditions of Western Siberia Lowland. Nauka, Moscow, 214 pp. (in Russian).

Brooker, A., Fraser, R.H., Olthof, I. et al., 2014. Mapping the activity and evolution of retrogressive thaw slumps by tasselled cap trend analysis of a Landsat satellite image stack. Permafrost and Periglacial Processes XXV (4), 243–256.

Burn, C.R., 2000. The thermal regime of a retrogressive thaw slump near Mayo, Yukon Territory. Can. J. Earth Sciences, XXXVII (7), 967–981.

Burn, C.R., Friele, P.A., 1989. Geomorphology, vegetation succession, soil characteristics and permafrost in retrogressive thaw slumps near Mayo, Yukon Territory. Arctic, XLII (1), 31–40.

Dvornikov, Y.A., Leibman, M.O., Khomutov, A.V. et al., 2019. Gas emission craters of the Yamal and Gydan peninsulas: A proposed mechanism for lake genesis and development of permafrost landscapes. Permafrost and Periglacial Processes XXX (3), 146–162.

Ecological Atlas of the Yamalo-Nenets Autonomous Okrug: results of scientific research, state, dynamics, forecast, 2018. E.V. Aghbalyan, R.I. Idrisov, A.V. Dobryakova (Eds.). Tyumen University Press, Tyumen, 116 pp. (in Russian).

Yershov E.D. (Ed.), 1989. Geocryology of the USSR. Western Siberia. Nedra, Moscow, 454 pp. (in Russian).

French, H.M., 2017. The periglacial environment. John Wiley & Sons, Hoboken, NJ, 544 pp.

Gubarkov, A.A., Leibman, M.O., 2010. Bead-shaped channel forms as evidence of paragenesis of cryogenic and hydrological processes in the small-river valleys of Central Yamal. Kriosfera Zemli [Earth's Cryosphere], XIV (1), 41–49.

Huang, L., Luo, J., Lin, Z. et al., 2020. Using deep learning to map retrogressive thaw slumps in the Beiluhe region (Tibetan Plateau) from CubeSat images. Remote Sensing of Environ. CCXXXVII, p. 111534.

Khomutov, A.V., Leibman, M.O., 2008. Landscape controls of Thermodenudation rate change on Yugorsky peninsula coast. Kriosfera Zemli [Earth's Cryosphere], XII (4), 24–35.

Khomutov, A.V., Leibman, M.O., Andreeva, M.V., 2012. Mapping of ground ice in Central Yamal. Vestnik Tumenskogo gosudarstvennogo universiteta [Tyumen State University Herald], No. 7, 76–84.

Khomutov, A., Leibman, M., Dvornikov, Y. et al., 2017. Activation of cryogenic earth flows and formation of thermocirques on central Yamal as a result of climate fluctuations. In: Workshop on World Landslide Forum. Cham, Springer, pp. 209–216.

Kizyakov, A.I., 2005. The dynamics of thermodenudation processes at the Yugorsky Peninsula coast. Kriosfera Zemli [Earth's Cryosphere], IX (1), 63–67.

Kokelj, S.V., Lacelle, D., Lantz, T.C. et al., 2013. Thawing of massive ground ice in mega slumps drives increases in stream sediment and solute flux across a range of watershed scales. J. Geophys. Research: Earth Surface, CXVIII (2), 681–692.

Kokelj, S.V., Lantz, T.C., Kanigan, J. et al., 2009. Origin and polycyclic behaviour of tundra thaw slumps, Mackenzie Delta region, Northwest Territories, Canada. Permafrost and Periglacial Processes XX (2), 173–184.

Lacelle, D., Brooker, A., Fraser, R.H., Kokelj, S.V., 2015. Distribution and growth of thaw slumps in the Richardson Mountains–Peel Plateau region, northwestern Canada. Geomorphology CCXXXV, 40–51.

Lantuit, H., Pollard, W.H., 2005. Temporal stereophotogrammetric analysis of retrogressive thaw slumps on Herschel Island, Yukon Territory. Natural Hazards and Earth System Sciences, V (3), 413–423.

Leibman, M.O., Egorov, I.P., 1996. Climatic and environmental controls of cryogenic landslides, Yamal, Russia. In: International Symposium on landslides terrain (Trondheim, June 17, 1996), Trondheim, Norway, pp. 1941–1946.

Leibman, M.O., Kizyakov, A.I., 2007. Cryogenic landslides of the Yamal and Yugorsky Peninsulas. IKZ SO RAN, Moscow, 206 pp. (in Russian).

Lewkowicz, A.G., 1987. Headwall retreat of ground-ice slumps, Banks Island, Northwest Territories. Can. J. Earth Sciences, 1987, 24 (6), 1077–1085.

Lewkowicz, A.G., Way, R.G., 2019. Extremes of summer climate trigger thousands of thermokarst landslides in a High Arctic environment. Nature Communication, X (1), 1–11.

Ramage, J.L., Irrgang, A.M., Herzschuh, U. et al., 2017. Terrain controls on the occurrence of coastal retrogressive thaw slumps along the Yukon Coast, Canada. J. Geophys. Research: Earth Surface, CXXII (9), 1619–1634.

Romanenko, F.A., 1997. Formation of lake basins on the plains of Arctic Siberia: Abstract of PhD thesis, Moscow, 25 pp. (in Russian).

Romanenko, F.A., Voskresensky, K.S., Tarasov, P.E. et al., 2001. Peculiarities of formation of relief and sediments West Yamal and Baidaratskaya Bay cost (Kara Sea). In: Problems of General and Applied Geoecology of the North. Moscow University Press, Moscow, pp. 41–68 (in Russian).

Segal, R.A., Lantz, T.C., Kokelj, S.V., 2016. Acceleration of thaw slump activity in glaciated landscapes of the Western Canadian Arctic. Environ. Res. Letters, XI (3), 034025.

Stepanov, M.N., Shavrin, A.V., 2005. Statistical Methods of Processing Mechanical Test Results. Mashinostroenie, Moscow, 399 pp. (in Russian).

Streletskaya, I.D., Ukraintseva, N.G., Drozdov, I.D., 2002. Tabular ground ice of the Arctic. A digital database. Vestnik Moskovskogo Universiteta. Seria 5. Geografia [Moscow University Bulletin. Series 5. Geography], No. 3, 7–13.

Voskresenskij, K.S., 2001. The Modern Relief-Forming Processes on Plains of the Northern Russia. Moscow University Press, Moscow, 262 pp. (in Russian).

Wang, B., Paudel, B., Li, H., 2016. Behaviour of retrogressive thaw slumps in northern Canada–three-year monitoring results from 18 sites. Landslides XIII (1), 1–8.

URL: http://yandex.ru/maps (last visited: 18.08.2019).

Received December 28, 2020
Revised September 15, 2021
Accepted October 14, 2021

Translated by N.B. Nesterova